

Research on an Improved Terrain Aided Positioning Model

Li Shidan

Dept. Electronic Engineering, Tsinghua University, Beijing, China
Email: lisd06@mails.tsinghua.edu.cn

Sun Liguo, Li Xin, Wang Desheng

Dept. Electronic Engineering, Tsinghua University, Beijing, China
Email: {slg00, xinli05, wangdsh_ee}@mails.tsinghua.edu.cn

Abstract—Terrain aided positioning (TAP) is a kind of positioning method which acquires position information from the terrain elevation datum underneath the vehicle. This method has the characteristics of autonomy, all-weather, anti-interference, strong stealthiness and high accuracy. It is widely used in the navigation system for various aircrafts, cruise missiles and underwater vehicles. The fundamentals of TAP is that it firstly measures the terrain elevation underneath the vehicle using relevant sensors, then compares these datum with the referenced Digital Elevation Map (DEM) and acquires the position information through matching algorithm. The system model for TAP currently used totally depends on the referenced DEM and the position acquired is the position referenced to the map rather than the true position. Due to the DEM error which is introduced during production procedure, the position on the map is not the real position. In order to overcome the problem, the paper proposes an improved TAP model which introduces the map error into the system model and gets the recursive solution based on the Bayesian framework which is numerically solved by RPF particle filter. From the simulation results, the new model has extraordinary performance for handling the error of DEM and the algorithm can estimate the map error and acquire the accurate position.

Index Terms—Terrain Aided Positioning, non-linear estimation, Bayesian iteration, Particle Filter, RPF

I. INTRODUCTION

Positioning and navigation system plays an important role on any vehicle no mater aerial, surface or underwater. The positioning system widely used nowadays can be divided into two categories: non-autonomy system and autonomy system.

Non-autonomy system, represented by the satellite based systems, such as GPS and GNSS can give accurate position information by receiving signals from external devices. These satellite based systems can easily be jammed by electromagnetic interference and even the

satellite itself may be attacked during war time. Meanwhile, due to the rapid attenuation of electromagnetic wave through sea water, such satellite based systems are not suitable for underwater vehicles.

Autonomy system, include inertial navigation system (INS) and terrain aided navigation system (TAN), does not need external devices for positioning and has the characteristics of all-weather, anti-interference, strong stealthiness and so on. They are widely used in many kinds of military vehicles for main or backup positioning system. Although INS can give high accurate positioning information during short time period, it has time accumulated errors which should be corrected by other systems, such as TAN or GPS, during work time, while the positioning error of TAN system mainly depends on the complexity and similarity of the terrain. TAN can also give high accurate position information from rugged terrain. For example, the TERPROM system widely used on NATO's military aircrafts has horizontal position accuracy of 10~25 meters [1].

From the introduction above, it can be inferred that the autonomy poisoning system, especially TAN system, plays an important role on military usage during war time and may be the only choice for underwater vehicles.

However the terrain aided positioning system currently used severely depends on the accuracy of the referenced Digital Elevation Map (DEM) which can be introduced with errors during producing [2] and finally leads to large differences between true position and estimated position. The paper just focuses on such problem and proposes an improved system model which introduces the map error components to the system model. The paper gives feasibility proof for the new model based on Bayesian theory and uses RPF particle filter for numerically getting the result. The simulation results confirm that the new model can estimate the map error and give more accurate position information compared to the basic model.

II. SYSTEM MODEL

The paper mainly discusses the terrain aided positioning system for aircrafts, but it can be easily extended to the underwater systems.

Manuscript received December 4, 2010; revised January 15, 2011; accepted January 26, 2011.

The airborne sensors for measuring terrain underneath the aircrafts are composed of barometric altimeter and radar altimeter. Fig. 1 shows the measurement procedure. The barometric altimeter measure the aircraft's altitude above sea level while the radar altimeter gets the elevation above the ground, and the difference between the two makes the terrain elevation underneath the vehicle. During the measuring, the pressure fluctuation and atmospheric turbulence may affect the barometric altimeter while the terrain roughness and the ground vegetation may influence the radar altimeter. There are several papers discussed such error aspects [3, 4, 5]. This paper concentrates on the influence caused by the DEM error and does not introduce the sensor error components into the system model.

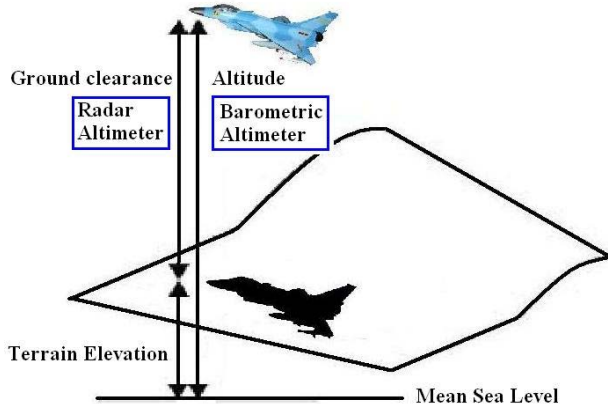


Figure 1. Terrain elevation measurement.

The basic model for terrain aided positioning is

$$\begin{cases} \mathbf{e}_{k+1}^* = \mathbf{e}_k^* + \mathbf{w}_k \\ \mathbf{x}_k = \mathbf{x}_k^* + \mathbf{e}_k^* \\ y_k = h^*(\mathbf{x}_k^*) + v_k \end{cases} \quad (1)$$

where \mathbf{e}_k^* is the position error of INS at time k which is modeled as time accumulated error. \mathbf{x}_k is the horizontal position from INS which is the true position \mathbf{x}_k^* plus INS error \mathbf{e}_k^* . y_k is the terrain elevation measurement which is the true terrain elevation $h^*(\mathbf{x}_k^*)$ plus the measurement noise v_k . The process noise \mathbf{w}_k and measurement noise v_k are independent with each other and also independent with the state \mathbf{e}_k^* . They have Gaussian distribution $w_k \sim N(0, Q_k)$, $v_k \sim N(0, R_k)$.

Due to the strong non-linearity of the terrain $h^*(\cdot)$, this model is classified into the non-linear model and the terrain aided positioning belongs to the typical non-linear estimation problem.

In the basic model above, $h^*(\cdot)$ represents the terrain elevation map. Because the map component is denoted as

$h^*(\mathbf{x}_k^*)$ in the measurement equation, the estimated position $\hat{\mathbf{x}}_k^*$ which is corrected by the $\hat{\mathbf{e}}_k^*$ through \mathbf{x}_k is the position referenced to the map $h^*(\cdot)$. That is to say, if $h^*(\cdot)$ is the real map then $\hat{\mathbf{x}}_k^*$ is the true position whereas if $h^*(\cdot)$ is the map with errors then $\hat{\mathbf{x}}_k^*$ is just the position on $h^*(\cdot)$ rather than the true position. Since the real map can not be acquired, the basic model can only estimate the position referenced to the map rather than the true position. Fig. 2 depicts the relationship of the values in the procedure. From the correction by the TAN, the system can give the relative position between the aircraft and the mountain and the error of that position compared to the true position is just the map error. Usually the relative position is enough for anti-collision usages. However the true position is also preferred in many occasions. So a more complicated model should be built to estimate the map error from time to time. Hence, we need to introduce the map error into the system model.

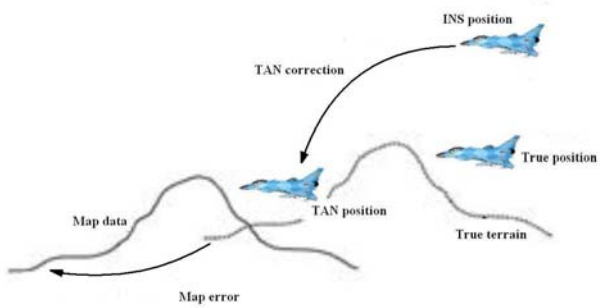


Figure 2. Relationship of the values in TAN.

To make the discussion simple, we assume that the map errors have the regional stability, thus they can be treated as constant parameters in a certain area.

Let $\Delta\mathbf{H}_k$, ΔV_k be the horizontal and vertical errors of terrain elevation map respectively where $\Delta\mathbf{H}_k$ composes of two components of x and y directions. Then the TAN referenced elevation map can be expressed as

$$h(\mathbf{x}_k^*) = h^*(\mathbf{x}_k^* + \Delta\mathbf{H}_k) + \Delta V_k \quad (2)$$

where $h^*(\cdot)$ represents the real terrain elevation map, \mathbf{x}_k^* is the real position.

Let $\mathbf{x} = \mathbf{x}_k^* + \Delta\mathbf{H}_k$, substitute to equation (2), we get

$$h^*(\mathbf{x}) = h(\mathbf{x} - \Delta\mathbf{H}_k) - \Delta V_k \quad (3)$$

Substitute (3) to the basic model (1), we get the new measurement equation using $h(\cdot)$ as

$$y_k = h(\mathbf{x}_k^* - \Delta\mathbf{H}_k) - \Delta V_k + v_k \quad (4)$$

Then we can get the new system model containing the map error components:

$$\begin{cases} \mathbf{e}_{k+1}^* = \mathbf{e}_k^* + \mathbf{w}_k \\ \Delta \mathbf{H}_{k+1} = \Delta \mathbf{H}_k \\ \Delta V_{k+1} = \Delta V_k \\ \mathbf{x}_k = \mathbf{x}_k^* + \mathbf{e}_k^* \\ y_k = h(\mathbf{x}_k^* - \Delta \mathbf{H}_k) - \Delta V_k + v_k \end{cases} \quad (5)$$

where equations $\Delta \mathbf{H}_{k+1} = \Delta \mathbf{H}_k$ and $\Delta V_{k+1} = \Delta V_k$ are the reflections of the assumption above, meaning that the error components are constant in the area concerned.

The compact form of (5) is

$$\begin{cases} \mathbf{e}_{k+1} = \mathbf{e}_k + \mathbf{w}_k \\ \mathbf{x}_k = \mathbf{x}_k^* + \mathbf{F} \cdot \mathbf{e}_k \\ y_k = h(\mathbf{x}_k^* - \Delta \mathbf{H}_k) - \Delta V_k + v_k \end{cases} \quad (6)$$

$$\text{where } \mathbf{e}_k = \begin{bmatrix} \mathbf{e}_k^* \\ \Delta \mathbf{H}_k \\ \Delta V_k \end{bmatrix}, \quad \mathbf{F} = \begin{bmatrix} 1 & 0 & 0 & 0 & 0 \\ 0 & 1 & 0 & 0 & 0 \end{bmatrix}, \quad \mathbf{w}_k = \begin{bmatrix} w_k \\ \mathbf{0} \\ 0 \end{bmatrix}.$$

III. RECURSIVE BAYESIAN ESTIMATION

According to Bayesian theory, a Bayesian estimation problem is defined by the joint density of the parameters and the observations, $p(x, y) = p(y|x)p(x)$. The estimator under the minimum mean square error criterion is the posterior mean $\hat{x}_{MS} = \int_{R^n} xp(x|y)dx$ [6]. So if there exists some relationship between the observation and the parameter, then the parameter can be estimated by the observation. From the information theory's point of view, the observation contains the information of the parameter when there exists stochastic relationship between the two. So we can make use of the observation to estimate the parameter.

Let \mathbf{Y}_k be the augmented measurement vector consisting of all the measurements up to time step k. From Bayesian formula [6] and the new system model (6), we have the posterior probability density function update:

$$\begin{aligned} p(\mathbf{e}_k | \mathbf{Y}_k) &= \frac{p(y_k | \mathbf{e}_k, \mathbf{Y}_{k-1}) \cdot p(\mathbf{e}_k | \mathbf{Y}_{k-1})}{p(y_k | \mathbf{Y}_{k-1})} \\ &= \alpha_k^{-1} \cdot p_{v_k}(y_k - h(\mathbf{x}_k^* - \mathbf{e}_k^* - \Delta \mathbf{H}_k) + \Delta V_k) \cdot p(\mathbf{e}_k | \mathbf{Y}_{k-1}) \end{aligned} \quad (7)$$

where

$$\alpha_k = \int_{R^N} p_{v_k}(y_k - h(\mathbf{x}_k^* - \mathbf{e}_k^* - \Delta \mathbf{H}_k) + \Delta V_k) \cdot p(\mathbf{e}_k | \mathbf{Y}_{k-1}) \cdot d\mathbf{e}_k.$$

The priori probability density function update is

$$\begin{aligned} p(\mathbf{e}_{k+1} | \mathbf{Y}_k) &= \int_{R^N} p(\mathbf{e}_{k+1} | \mathbf{e}_k, \mathbf{Y}_k) \cdot p(\mathbf{e}_k | \mathbf{Y}_k) \cdot d\mathbf{e}_k \\ &= \int_{R^N} p_{w_k}(\mathbf{e}_{k+1}^* - \mathbf{e}_k^*) \cdot p(\mathbf{e}_k | \mathbf{Y}_k) \cdot d\mathbf{e}_k \end{aligned} \quad (8)$$

Given the initial prior density $p(\mathbf{e}_0 | \mathbf{Y}_{-1}) = p(\mathbf{e}_0)$, we can recursively generate the posterior probability density through equation (7) and (8). And the state

estimate is $\hat{\mathbf{e}}_k = E[\mathbf{e}_k | \mathbf{Y}_k]$ with covariance matrix $\hat{\mathbf{P}}_k = E[(\mathbf{e}_k - \hat{\mathbf{e}}_k) \cdot (\mathbf{e}_k - \hat{\mathbf{e}}_k)^T | \mathbf{Y}_k]$.

The recursive Bayesian equations above are the theoretical solution for model (6) and are intractable due to the complexities of the posterior and priori probability density function in the non-linear model. Usually the numerical methods should be used for calculating the result, such as point mass filter (PMF) or particle filter (PF). This paper uses the PF to solve the model.

IV. PARTICAL FILTER

The fundamental of particle filter is to use particles with weights for representing the probability density function (PDF) and uses the recursion of the particle set to replace the recursion of the posterior density function. When the complex probability density function is represented by the particle set the integration in α_k and (8) can be easily calculated according to Monte Carlo integration theory.

Let $\{\mathbf{e}_k^i, w_k^i\}_{i=1}^M$ be particle set for the posterior PDF

$$p(\mathbf{e}_k | \mathbf{Y}_k), \text{ where } \sum_{i=1}^M w_k^i = 1, \text{ then}$$

$$p(\mathbf{e}_k | \mathbf{Y}_k) \approx \sum_{i=1}^M w_k^i \cdot \delta(\mathbf{e}_k - \mathbf{e}_k^i) \quad (9)$$

where $\delta(\cdot)$ is Dirac-Delta function. The estimator and its covariance are

$$\begin{aligned} \hat{\mathbf{e}}_k &= E[\mathbf{e}_k | \mathbf{Y}_k] \\ &= \int_{R^N} \mathbf{e}_k \cdot \sum_{i=1}^M w_k^i \cdot \delta(\mathbf{e}_k - \mathbf{e}_k^i) \cdot d\mathbf{e}_k \\ &= \sum_{i=1}^M w_k^i \cdot \mathbf{e}_k^i \end{aligned} \quad (10)$$

$$\begin{aligned} \hat{\mathbf{P}}_k &= E[(\mathbf{e}_k - \hat{\mathbf{e}}_k) \cdot (\mathbf{e}_k - \hat{\mathbf{e}}_k)^T | \mathbf{Y}_k] \\ &= \int_{R^N} (\mathbf{e}_k - \hat{\mathbf{e}}_k) \cdot (\mathbf{e}_k - \hat{\mathbf{e}}_k)^T \cdot \sum_{i=1}^M w_k^i \cdot \delta(\mathbf{e}_k - \mathbf{e}_k^i) \cdot d\mathbf{e}_k \\ &= \sum_{i=1}^M w_k^i \cdot (\mathbf{e}_k^i - \hat{\mathbf{e}}_k) \cdot (\mathbf{e}_k^i - \hat{\mathbf{e}}_k)^T \end{aligned} \quad (11)$$

The recursion of the particle set is simply explained below:

Let $\{\mathbf{e}_{k-1}^i, w_{k-1}^i\}_{i=1}^M$ be the particle set at time k-1 which represents the posterior PDF $p(\mathbf{e}_{k-1} | \mathbf{Y}_{k-1})$. At time k, we first draw sample \mathbf{e}_k^i from an easy sampling distribution $q(\mathbf{e}_k | \mathbf{e}_{k-1}^i, y_k)$ and then update its weight using

$$w_k^i \propto w_{k-1}^i \cdot \frac{p(y_k | \mathbf{e}_k^i) \cdot p(\mathbf{e}_k^i | \mathbf{e}_{k-1}^i)}{q(\mathbf{e}_k^i | \mathbf{e}_{k-1}^i, y_k)} \quad (12)$$

Then the new particle set $\{\mathbf{e}_k^i, w_k^i\}_{i=1}^M$ represents the posterior PDF $p(\mathbf{e}_k | \mathbf{Y}_k)$. Thereby this simple particle set recursion takes place of the intractable recursion of the posterior PDF.

The distribution $q(\mathbf{e}_k | \mathbf{e}_{k-1}^i, y_k)$ is called importance sampling density function which can be selected according to requirements. Usually for convenient usage, the state transition PDF $p(\mathbf{e}_k | \mathbf{e}_{k-1}^i)$ is chosen [7]. Substitute $p(\mathbf{e}_k | \mathbf{e}_{k-1}^i)$ into (12) yields

$$w_k^i \propto w_{k-1}^i \cdot p(y_k | \mathbf{e}_k^i) \quad (13)$$

Because the last three components of the state vector in the new model are constant parameters, we need special treatment for random components and constant components respectively during particle recursion. We use important sampling density function for random components and leave constant components unchanged during particle transition:

$$\mathbf{e}_k^i = \begin{bmatrix} \mathbf{e}_k^{*i} \sim p(e_k^* | e_{k-1}^*) \\ \Delta \mathbf{H}_k^i = \Delta \mathbf{H}_{k-1}^i \\ \Delta V_k^i = \Delta V_{k-1}^i \end{bmatrix} \quad (14)$$

$$p(e_k^* | e_{k-1}^*) \sim N(e_{k-1}^*, Q_k) \quad (15)$$

$$p(y_k | \mathbf{e}_k^i) = p_{y_k}(y_k - h(\mathbf{x}_k - \mathbf{e}_k^i - \Delta \mathbf{H}_k^i) + \Delta V_k^i) \quad (16)$$

Equations (13) to (16) finally accomplish the particle filter recursion for map error model (6).

In order to decrease the impacts on PF performance caused by the phenomenon of particle degeneracy and particle collapse, we need some resampling scheme for effective representing the PDF.

Since our new model (6) consists constant parameter which can be seen as random variable with extremely small process noise, common particle filters such as SIS, ASIR are not suitable for handling the model with small process noise states which can lead to severe particle degeneracy phenomenon due to the lose of particle diversity [7]. In this paper, we chose Regularized Particle Filter (RPF) [8] for resampling which can maintain the particle diversity to the maximum extent.

During resampling, we actually resample from the discrete distribution

$$p(\mathbf{e}_k | \mathbf{Y}_k) \approx \sum_{i=1}^M w_k^i \cdot \delta(\mathbf{e}_k - \mathbf{e}_k^i) \quad (17)$$

which makes that the new samples cannot get rid of the old particle set and leads to singular composition after several iterations. The main idea of RPF is to make the PDF continuous by introducing kernel function and let the particle evolve in the continuous space. The resampling distribution function for RPF is

$$p(\mathbf{x}_k | \mathbf{Y}_k) \approx \sum_{i=1}^M w_k^i \cdot K_h(\mathbf{x}_k - \mathbf{x}_k^i) \quad (18)$$

$$K_h(\mathbf{x}) = \frac{1}{h^{n_x}} K\left(\frac{\mathbf{x}}{h}\right) \quad (19)$$

where n_x is the dimension of \mathbf{x} , $h > 0$ is the bandwidth of kernel function $K(\cdot)$. $K(\cdot)$ can be seen as a symmetric probability density function on \mathbf{R}^{n_x} and $K_h(\cdot)$ is called the rescaled kernel.

The kernel and the bandwidth are chosen so as to minimize the mean integrated square error between the true posterior density and the corresponding regularized weighted empirical measure in (18). In a special case of equally weighted sample, the optimal choice of the kernel is the Epanechnikov kernel [8]. To reduce computing cost, we use Gaussian kernel instead and the corresponding optimal bandwidth is [9]

$$h_{opt} = A \cdot N^{-\frac{1}{n_x+4}} \quad (20)$$

$$\text{with } A = (4/(n_x + 2))^{\frac{1}{n_x+4}}.$$

For implement, the new particle set can be generated by

$$\mathbf{x}_k^{i*} = \mathbf{x}_k^i + h_{opt} \mathbf{D}_k \boldsymbol{\epsilon}^i \quad (21)$$

where \mathbf{D}_k is the square root of the empirical covariance matrix of the samples $\{\mathbf{x}_k^i, w_k^i\}_{i=1}^M$. $\boldsymbol{\epsilon}^i$ is the sample drawn from the kernel function.

The resampling procedure of RPF is

-
- Calculate the effective number of particles N_{eff} [10]
 - IF $N_{eff} < N_{thr}$
 - Calculate the empirical covariance matrix \mathbf{S}_k for particle set $\{\mathbf{x}_k^i, w_k^i\}_{i=1}^M$
 - Calculate the square root \mathbf{D}_k of \mathbf{S}_k
 - Resample the particle set using Systematic Resampling [11] method, and get the new set $\{\mathbf{x}_k^i, w_k^i, -\}_{i=1}^M$
 - FOR i=1:M
 - ✧ Draw sample $\boldsymbol{\epsilon}^i$ from kernel
 - ✧ Update particle $\mathbf{x}_k^{i*} = \mathbf{x}_k^i + h_{opt} \mathbf{D}_k \boldsymbol{\epsilon}^i$
 - END FOR
 - END IF
-

V. SIMULATION RESULTS

The reference DEM data for the simulation is from ASTER GDEM produced by METI and NASA, which has grid size of 30 meters [12]. The area we use is between 40 and 41 degrees latitude north and 105 and 106 degrees longitude west.

In our simulation, we use the DEM from ASTER GDEM to be the real terrain $h^*(\cdot)$ and add some map errors to get the reference DEM used for filtering. We use bilinear interpolation method to draw elevation data from the grid map.

The simulation procedure is as follows:

Step 1, chose a trajectory on the real map to be the reference trajectory and get $\{\mathbf{x}_k^*\}_{k=1}^N$.

Step 2, get the output of the INS $\{\mathbf{x}_k\}_{k=1}^N$ by equation

$$\begin{cases} \mathbf{e}_{k+1}^* = \mathbf{e}_k^* + \mathbf{w}_k \\ \mathbf{x}_k = \mathbf{x}_k^* + \mathbf{e}_k^* \end{cases}$$
 and the initial INS error \mathbf{e}_0^* .

Step 3, given the initial distribution of state $p(\mathbf{e}_0)$, we can get estimate $\{\hat{\mathbf{e}}_k\}_{k=1}^N$ through RPF particle filter and acquire $\{\hat{\mathbf{x}}_k\}_{k=1}^N$ using equation $\hat{\mathbf{x}}_k^* = \mathbf{x}_k - \hat{\mathbf{e}}_k^*$.

Step 4, repeat Step 2 and Step 3 to do Monte Carlo simulation several times and get average estimation error to evaluate the system performance.

The map errors used in our simulation are $\Delta\mathbf{H} = [200, 150]^T$, $\Delta V = 30$.

The DEM and the flight path used are depicted in Fig. 3. This area has a mountain from north to south and the flight path we chose is a uniform speed trajectory with a turn round in the middle of the path. Fig. 3 shows an estimated result for map error model.

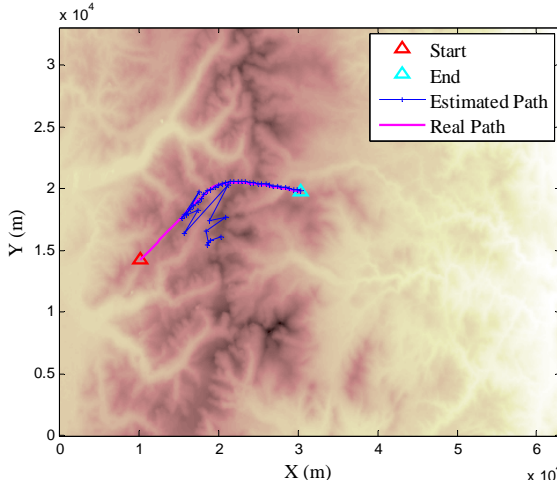


Figure 3. Flight path and estimation result for map error model.

Fig. 4 is the average root mean square error (RMSE) curve for horizontal position estimation which is generated by using 100 Monte Carlo simulations. The solid line is the RMSE of the map error model while the dash line is for the basic model. Because the map error model actually estimates the map errors and corrects the position with them, so it can get more accurate position information. From the figure, the horizontal RMSE of the new model is about 200 meters smaller than the basic model which is close to the horizontal map error we set,

thus confirms the new model's capability of map error estimation. However, the new model has much slower convergence speed than the basic model which may caused by the high dimensionality of the state vector in the new model.

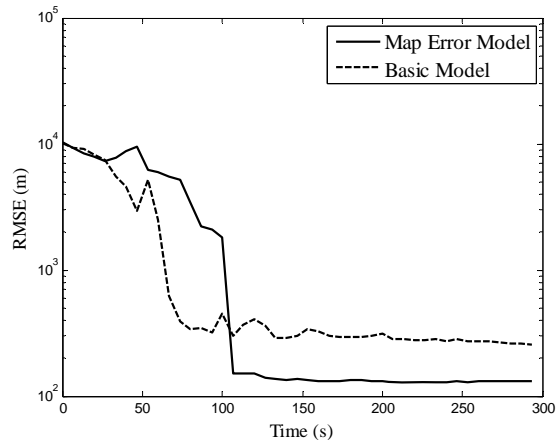


Figure 4. Horizontal RMSE with MC=100.

Fig. 5 shows the terrain elevation estimation error for both map error model and the basic model. The terrain elevation estimation for map error model is acquired by

$$h^*(\mathbf{x}_k^*) \approx h(\hat{\mathbf{x}}_k^* - \Delta\mathbf{H}_k) - \Delta V_k \quad (22)$$

where $\hat{\mathbf{x}}_k^* = \mathbf{x}_k - \hat{\mathbf{e}}_k^*$, while for basic model

$$h^*(\mathbf{x}_k^*) \approx h(\hat{\mathbf{x}}_k^*). \quad (23)$$

Apparently, the new model takes map errors (both horizontal and vertical error) into consideration and uses the estimated error to correct the measurement while the basic model just depends on the map itself. So from the simulation results shown in Fig. 5, the error of basic model is about 20 meters higher than the new model which is close to the vertical error of the map we set.

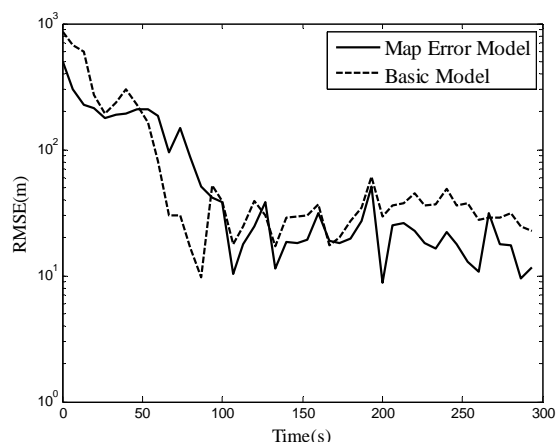


Figure 5. Terrain Elevation Estimation Error with MC=100.

Fig. 6 is the average map error estimate with 100 Monte Carlo simulations. The dash line is the true error while the solid curve is the estimated parameter. From the figure, the filter is best for the vertical error estimation which has rapid convergence, high accuracy and good stability. That because the vertical error component has a

linear structure in the system model that can be even extracted from the system model and use Kalman filter for solving, such as Rao-Blackwellize method [13]. So when using particle filter, such component with simple structure can be easily estimated. For horizontal map errors, the convergence of Y direction is worse than the X direction, that because the terrain in the second half path varies more on the X direction than Y direction which benefits the component estimation on X direction. Meanwhile, the convergent speed for horizontal errors is very slow which may caused by the constant characteristic of these states.

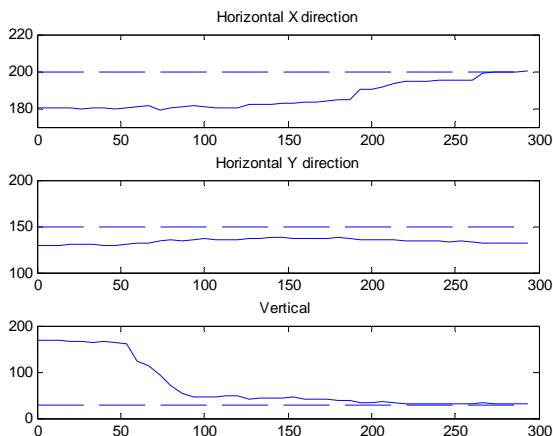


Figure 6. Map error estimation.

Fig. 7 and Fig. 8 show the particle evolution process for SIS and RPF respectively for comparison of the effectiveness of these two different algorithms. The figures show the histogram of one component of the state in the particle set at different time step which can be seen as the distribution of that component. The component we chose to show is the X direction error of the map error component which is a constant parameter in the state vector.

Fig. 7 is for SIS. As mentioned above, the commonly used particle filter is not suitable for solving the model with constant parameters. For these parameters the initial particle set at $k=1$ contains the whole data values for the evolution that there will be no new values generated in later time step since they have no process noise. So the initial distribution must cover the true value we estimated otherwise the filter can not give that value. From Fig. 7, after several iterations the distribution is concentrated to some distinct values and the state can hardly move to other values.

In Fig. 7, when $k=1$, the initial distribute is a Gaussian distribution with mean equal to 180 and can cover the true value of 200 which is the map error we set. After some iterations, the amount of effective values decreases and when $k=16$ there are only two bars in the histogram which do not contain the true value thus after that the filter can not give the accurate value of 200.

In SIS, since the parameter components in the particle do not change during state transition step, the degeneracy phenomenon of these components will affect the evolution of the other state components and lead to slow

convergent speed, low accuracy and even divergent when the particles fall into bad bars.

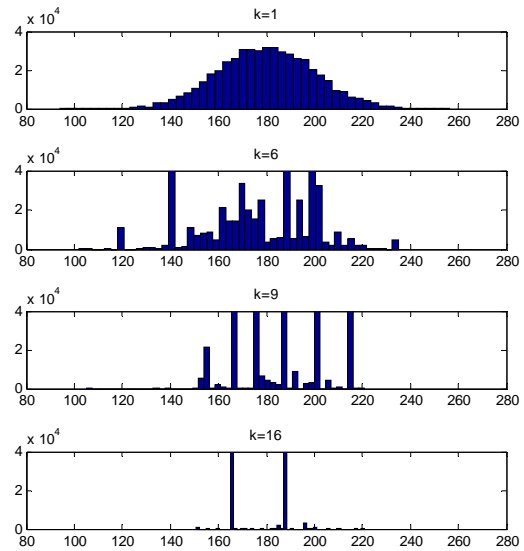


Figure 7. particle evolution for SIS.

Fig. 8 is for RPF. RPF uses an effective resampling scheme which draws new particles from a continuous distribution constructed from the discrete one. It can make the singular bar extent to a region according to some distribution which can generate new values during evolution. From Fig. 8, the distribution of the parameter moves towards the true value with time and concentrate to the true value when convergent.

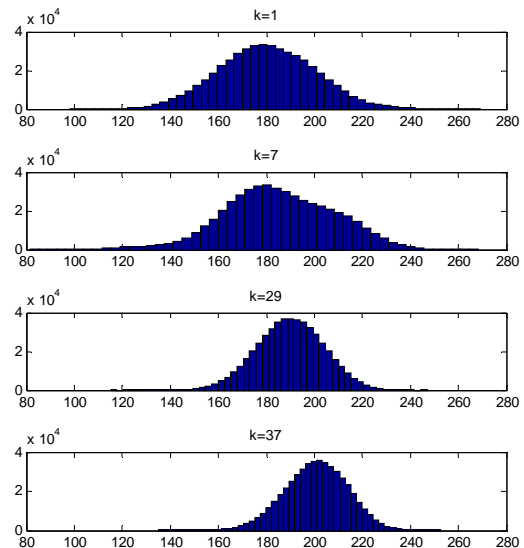


Figure 8. particle evolution for RPF.

In Fig. 8, the initial distribution is also Gaussian. When $k=7$, the mean of the parameter move away from 180 and the right side of the distribution expands. The mean becomes 190 when $k=29$ and finally gets to 200 which is the true value when $k=37$. During each time step, RPF

can maintain the particle diversity to the maximum extent and the particle set can move towards the right direction as long as the true value is covered by the distribution. However, this moving procedure is much slower than SIS.

According to the comparison above, the common SIS particle filter can hardly handle the constant parameter estimation in our model and the particle degenerate phenomenon always occurs after several iteration steps. When using the resampling scheme of RPF, the particle diversity can be maintained and the particle set can move to the true value. Meanwhile, we found that the constant parameter incorporated in the complex non-linear system is hard to estimate, the filter is slow on convergence speed and sensitive to the initial value.

V. CONCLUSION

In this paper, the system model of terrain aided positioning system is studied and an improved system model is proposed which overcomes the disadvantage of the dependency on the accuracy of the map that exists in the basic model. The new model can estimate map error and correct the position to acquire more accurate position information. The paper selects particle filter for this nonlinear model and compares the performance of SIS and RPF particle filters. From our simulation, the RPF has much better performance for our new model which contains constant parameter in the state vector. With RPF, our simulation results confirm the better performance of the new model than the basic model that the accuracy of the horizontal position estimation is improved by around 200 meters which is close to the map error we set.

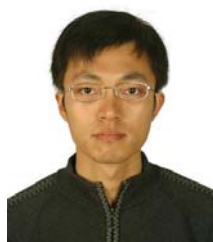
With this map error model, our terrain aided positioning system can give actual position information other than just the position on the map. This progress will make the system more preferable for use.

ACKNOWLEDGMENT

We should thank Jia Ke for his DEM data acquisition and preprocessing work. And we also appreciate the institutions of METI and NASA for their opening support of ASTER GDEM datum.

REFERENCES

- [1] M. Cowie, and N. Wilkinson, "Latest development of the TERPROM (R) Digital Terrain System (DTS)," *2008 Ieee/Ion Position, Location and Navigation Symposium*, Vols 1-3: 658-668, 2008.
- [2] K. J. Markham, and W. A. Morris, "Digital terrain elevation models produced using radar altimetry and GPS data," *Igarss 2002: Ieee International Geoscience and Remote Sensing Symposium and 24th Canadian Symposium on Remote Sensing*, Vols I-Vi, Proceedings: 2723-2725, 2002.
- [3] K. B. Anonsen, and O. Hallingstad, "Terrain aided underwater navigation using point mass and particle filters," *2006 IEEE/ION Position, Location and Navigation Symposium*, Vols 1-3: 1027-1035, 2006.
- [4] P. J. Nordlund, and F. Gustafsson, "Recursive Estimation of 3-Dimensional Aircraft Position Using Terrain-Aided Positioning," Linkoping, 2001.
- [5] P. Frykman, "Applied particle filters in integrated aircraft navigation," *Electrical Engineering*, Linkoping University, 2003.
- [6] J. M. Bernardo, and A. F. M. Smith, *Bayesian Theory*, 2nd ed., New York: Wiley, 1998.
- [7] B. Ristic, S. Arulampalam, and N. Gordon, *Beyond the Kalman Filter*, Artech House, Boston, London, 2004.
- [8] B. W. Silverman, "Density Estimation for Statistics and Data Analysis," Vol. 26 of *Monographs on Statistics and Applied Probability*, Chapman & Hall, London, 1986
- [9] C. Musso, N. Oudjane, and F. LeGland, "Improving regularised particle filters," in *Sequential Monte Carlo Methods in Practice*, New York: Springer, 2001.
- [10] A. Kong, J. S. Liu, and W. H. Wong, "Sequential imputations and Bayesian missing data problems," *Journal of the American Statistical Association*, vol. 89, no. 425, pp. 278-288, 1994.
- [11] G. Kitagawa, "Monte Carlo filter and smoother for non-Gaussian non-linear state space models," *Journal of Computational and Graphical Statistics*, vol.5, no. 1, pp. 1-25, 1996.
- [12] "<http://asterweb.jpl.nasa.gov/>," January, 2011.
- [13] A. Doucet, N. d. Freitas, K. Murphy, and S. Russell, "Rao-Blackwellised particle filtering for dynamic bayesian networks," *Proceedings UAI2000*: 176-183, 2000.



Li Shidan, born in 1983, Ph. D. candidate in Department of Electronic Engineering, Tsinghua University. His research interests mainly focus on particle filters, navigation technique and radar signal processing. He is currently doing research at the High-speed Signal Processing and Network Transmission Institute in Tsinghua University. He has participated in the terrain aided navigation project and the marine navigation radar system project.

Sun Liguo, born in 1982, Ph. D. candidate in Department of Electronic Engineering, Tsinghua University. His research areas include navigation and positioning technique, signal processing on Geographic Information System.

Li Xin, born in 1967, Ph. D. candidate in Department of Electronic Engineering, Tsinghua University. Her interests focus on the target tracking technique and aircraft's navigation system.

Wang Desheng, born in 1946, Prof. in Department of Electronic Engineering, Tsinghua University. He is doing research on signal processing and framework techniques on radar display and control terminal. He is one of the first for developing raster scan radar terminal and the frequency jumper radar system.